ADVANCED FUNCTIONAL MATERIALS

DOI: 10.1002/adfm.200800333

Fabrication of Reversibly Crosslinkable, 3-Dimensionally Conformal Polymeric Microstructures**

By *Luke A. Connal, Robert Vestberg, Craig J. Hawker,* and *Greg G. Qiao**

Multifaceted porous materials were prepared through careful design of star polymer functionality and properties. Functionalized core crosslinked star (CCS) polymers with a low glass transition temperature (T_g) based on poly(methyl acrylate) were prepared having a multitude of hydroxyl groups at the chain ends. Modification of these chain ends with 9-anthracene carbonyl chloride introduces the ability to reversibly photocrosslink these systems after the star polymers were self-assembled by the breath figure technique to create porous, micro-structured films. The properties of the low T_g CCS polymer allow for the formation of porous films on non-planar substrates without cracking and photo-crosslinking allows the creation of stabilized honeycomb films while also permitting a secondary level of patterning on the film, using photo-lithographic techniques. These multifaceted porous polymer films represent a new generation of well-defined, 3D microstructures.

1. Introduction

The direct correlation between 3D polymer structure and properties is allowing a range of new materials to be prepared with diverse applications.[1,2] Specifically designed macromolecular architectures are in turn enabled by controlled polymerization techniques where the choice of monomer (e.g., acrylate or methacrylates), polymer architecture (e.g., linear or star), and the end group functionalities can now all be tailored for a specific purpose. This becomes particularly important when synthesizing polymers for demanding applications, where stringent requirements on processing and functionality are needed.

One such process, which has distinct requirements for the polymer precursor, is the preparation of porous films by the "breath figure" (BF) technique.[3] The BF technique relies on the precipitation of a polymer around a condensed water droplet (breath figure), initiated by rapid evaporation of a polymer solution in a humid environment. This technique introduces constraints on the polymers that can be used. For example, the polymer must be soluble in volatile organic solvents and must precipitate in water. This system has also been reported to be sensitive to polymer architecture – polymers capable of forming spherical structures in solution lead to superior performance.[2,4] Furthermore, for this process to deliver films with commercial value, more stringent requirements are necessary with polymer films that are non-brittle, solvent resistant, and easily functionalized are increasingly desired.

Recently we reported the successful formation of honeycomb films on the surface of TEM grids,[5] as well as on particulate surfaces.[6,7] This unique ability to pattern non-planar substrates was accomplished by utilizing a star polymer based on poly(dimethylsiloxane) which has an extremely low glass transition temperature ($T_g = -123\,^{\circ}C$). Subsequent surveying of a library of core crosslinked star (CCS) polymers with a range of T_g values showed that flexible honeycomb films, capable of contouring to non-flat substrates, can only be formed from star polymers with a T_g below ca. 50 °C.[8] This latest extension demonstrates the versatility of the technique and shows that a range of common polymers, with appropriate architectures, can form these flexible, and ordered porous films, on practically any surface. This low T_g method is very different to the confinement technique described by Park et al.[9] The technique presented here describes the preparation of flexible honeycomb films.

For these honeycomb materials to realize their potential in many applications, a higher degree of structural integrity is important, and crosslinking them chemically can greatly increase their applicability in a range of areas.[10–12] Crosslinked honeycomb films, on flat substrates, have been achieved via chemical[13–15] and UV[16,17] activated reactions. UV has an advantage as it is non-evasive and can be used to create further patterns in the films – extending their versatility.[18] We were

[*] Prof. G. G. Qiao, Dr. L. A. Connal
Polymer Science Group (PSG), Department of Chemical and Biomolecular Engineering
The University of Melbourne
Parkville, Victoria, 3010 (Australia)
E-mail: gregghq@unimelb.edu.au
Dr. R. Vestberg, Prof. C. J. Hawker
Materials Research Laboratory (MRL) and Departments of Materials Chemistry and Biochemistry, University of California
Santa Barbara, California 93106 (USA)

[**] The Authors would like to thank Dr. Alexander Zelikin, Dr. Angus Johnston and Dr. Will Mulholland for help with fluorescent microscopy. Financial support from an Australian Research Council's Discovery Grant (DP0345290) and the NSF MRSEC Program DMR-0520415 (MRL-UCSB) are gratefully acknowledged. The authors would also like to thank the Royal Australian Chemical Institute (Polymer Division) for travel support through the O'Donnell prize (L. A. C).

interested in extending the versatility of UV activated crosslinking reactions and creating reversibly crosslinkable systems. This strategy has the potential to open new areas of research and development that otherwise would not be feasible, from advanced patterning strategies to reversible biosensors. Our main interest was focused on the reversible crosslinking reaction of anthracene substituents through photo dimerization due to the reversible nature and orthogonality of the process coupled with the wide applicability of this generalized approach.

Anthracene and its derivatives undergo [4 + 4] photo-dimerization upon long-wave UV irradiation (>350 nm).[19,20] The dimer can be reversed to the original monomers (photo-scission) upon exposure to short-wave UV light (<300 nm). This versatile reaction has been demonstrated in diverse areas such as optical memory,[21–23] langmuir-blodgett monolayers,[24] biosensors,[25,26] and hydrogels.[27,28]

Herein, we report the preparation of an anthracene functional poly(methyl acrylate) CCS polymer by the ''arm first'' approach, utilizing atom transfer radical polymerization (ATRP). We demonstrate the formation of ordered honeycomb films on both 2D and 3D surfaces using this CCS polymer followed by reversible photo-crosslinking reactions. This combination of the ability to coat any non-planar surface, and the ability to crosslink, greatly increases the applicability of these films. It also allows the creation of multifaceted porous polymer films with three levels of patterning: ordered pores in a hexagonal pitch – originating from the BF technique, 3D patterns – from the honeycomb film conforming to a patterned substrate, and photo-rewritable patterns – through the dimerization of the anthracene moiety, using patterned masks.

2. Results and Discussion

The strategy for fabrication of micropatterned materials through the combination of orthogonal patterning techniques initially involved the preparation of chain end functionalized, core crosslinked star (CCS) polymers with a low T_g by an arm first strategy (Scheme 1).[29] This star polymer was then used to prepare honeycomb materials by the BF technique followed by reversible photo-dimerization of the anthracene groups at the chain ends to crosslink and stabilize the honeycomb films.

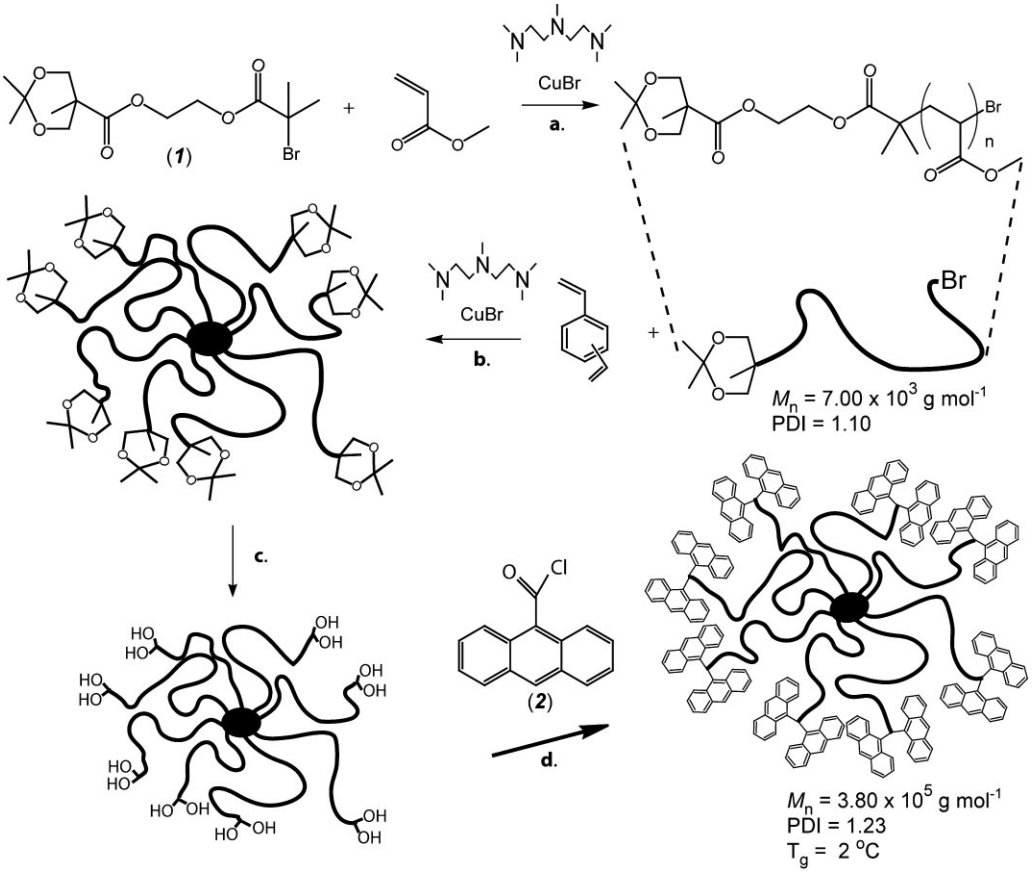

Scheme 1. Synthesis and functionalization of PMA CCS polymer with anthracene moiety. a) Bulk, 80 °C, 2 h. b) Anisole, 100 °C, 40 h. c) Dowex, H^+ resin, MeOH/THF, 12 h d) Dry THF, DMAP, pyridine, 18 h.

ADVANCED FUNCTIONAL MATERIALS

2.1. Synthesis of Anthracene Functional Star Polymer

To obtain a conformal system a low glass transition polymer based on PMA was chosen and the linear polymers were prepared by ATRP, utilizing the protected initiator 2-(2′-bromo-2′-methylpropanoyloxy)ethyl 2,2,5-trimethyl-1,3-dioxane-5-carboxylate (**1**) (Scheme 1a). The linear macroinitiator ($M_n = 7.0 \times 10^3$ g mol^{-1}, PDI = 1.10) was isolated and then reacted with divinyl benzene under ATRP conditions to form a CCS polymer with protected hydroxyl functionalities at the periphery ($M_n = 3.80 \times 10^5$ g mol^{-1}, PDI = 1.23) (Scheme 1b). This star polymer was analyzed by DSC and shown to have a T_g of 3 °C. The PMA star with acetonide end group was then dissolved in a THF/MeOH mixture and deprotected under acidic conditions (Dowex-50-X2) to yield star polymers with 2 hydroxyl groups per arm (Scheme 1c) which were reacted with 9-anthracene carbonyl chloride (**2**) in dry THF to yield the desired anthracene functional CCS polymer (Scheme 1d). The presence of the anthracene functionalities was confirmed by both ^{1}H NMR spectroscopy and UV spectroscopy which showed unique resonances in the aromatic region and the characteristic absorption profile for anthracene in the region from 330 nm to 400 nm (Fig. 1). The extent of chain end functionalization was calculated from UV spectroscopy and shown to be greater than 90% in which corresponds to approximately 70 anthracene groups at the periphery of the star.

2.2. Formation of Honeycomb Films

The anthracene functional star polymers were cast from benzene solution (10 mg mL^{-1}) under a flow of humid air (3 L min^{-1}, 70% relative humidity) to form honeycomb films. The polymers successfully formed ordered honeycomb films on planar substrates (data not shown). The use of the low T_g PMA as the macroinitiator allows the film to be cast onto non-flat surfaces[4–7] with Figure 2a and b displaying the anthracene functional honeycomb film contouring to the surface of a TEM grid (600 mesh, hexagonal pitch). The successful film formation on the TEM grid shows that the anthracene functionality does not alter the PMA based CCS polymer's ability to create flexible honeycomb films.

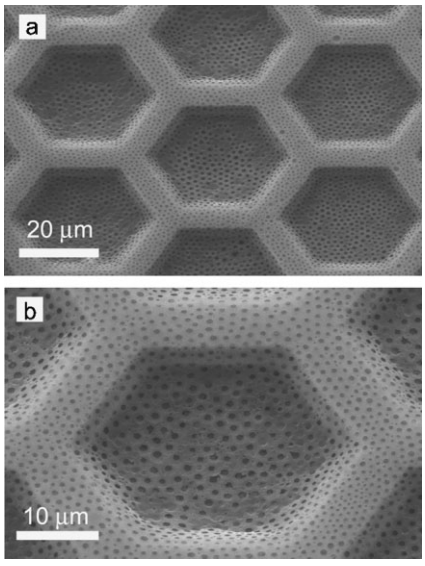

Figure 2. Images of honeycomb films cast from anthracene functional PMA star a) and b) SEM images of a honeycomb film cast on the surfaces of a hexagonal (600 mesh) TEM grid.

2.3. Reversible Photocrosslinking of the Honeycomb Films

Honeycomb films cast from anthracene functional stars were then used for the reversible photocrosslinking reaction through the [4 + 4] dimerization of the anthracene groups (Scheme 2). The reversible dimerization of the anthracene moiety is conveniently monitored by fluorescence spectrometry as there is a decrease in photoluminescence upon dimerization. The original fluorescence intensity was detected after the honeycomb film was formed by casting the anthracene functional star polymer solution (Fig. 3, original). This film was then irradiated under dimerization conditions (4 h, 366 nm) and the subsequent fluorescence detection showed a decrease in intensity (Fig. 3, point a1). Irradiation at 254 nm to promote the reverse

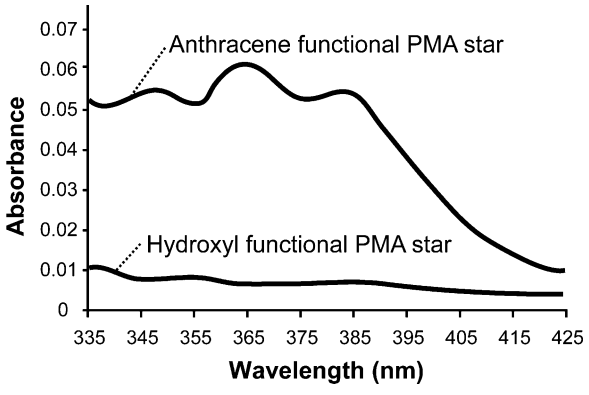

Figure 1. UV-Absorption spectra of anthracene end functional poly(methyl acrylate) (PMA) star polymer (top), and absorption spectra of hydroxyl functional PMA star polymer (bottom).

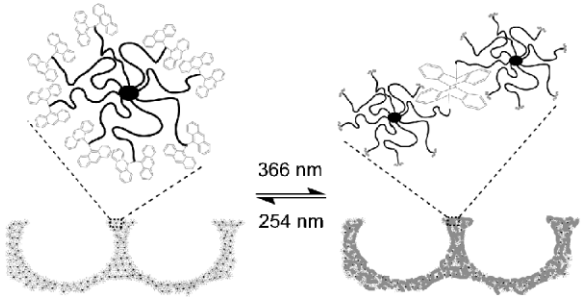

Scheme 2. Schematic representation of reversible photo-dimerization of anthracene functional star honeycomb films.

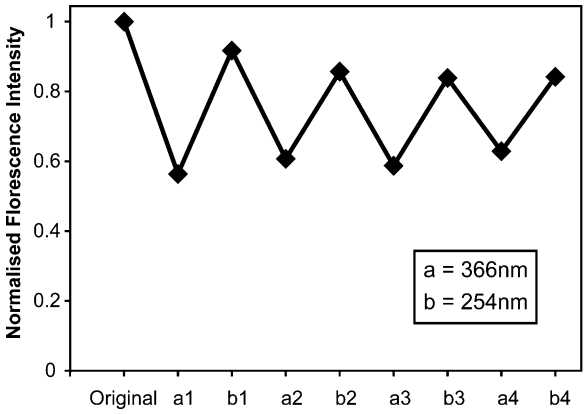

Figure 3. Normalized fluorescence intensity (integrated from 400–700 nm) of anthracene functional honeycomb film. Original; untreated, as cast honeycomb film; a) film crosslinked at 366 nm for 4 h; and b) film reversed back to uncrosslinked state by 254 nm light for 4 h. The crosslink, uncross-link cycle was repeated four times.

decrosslinking reaction (4 h, 254 nm) leads to an increase in the fluorescence which correlates with regeneration of the anthracene groups (Fig. 3, point b1). This cycle was completed four times and Figure 3 displays the success of repeated crosslinking and decrosslinking of the honeycomb morphology. The reduced magnitude of the fluorescence intensity after repeated cycles is possibly due to incomplete reversibility of the dimerization reaction.

To demonstrate the dimensional and mechanical stability of the crosslinked honeycomb film, a film was cast onto a TEM grid, crosslinked at 366 nm for 4 h, and washed several times with THF. Figure 4 shows the resulting honeycomb film on the TEM grid surface which retains the original structure with hexagonal arrays of 1–2 micrometers pore being clearly visible. This orthogonal crosslinked honeycomb film which is stable in the presence of both aqueous and organic solvents. To confirm the mechanism of film crosslinking a series of controlled experiments were performed. Two hydroxyl functional PMA star polymer films were cast and treated in alternate ways, one film was irradiated at 366 nm light while the other was not subjected to UV irradiation. Upon washing with THF both of these films completely dissolved. A further control experiment was performed with anthracene functional PMA star polymer, the film was cast and the washed with THF without UV irradiation; this film also completely dissolved upon washing. These controlled experiments confirm the mechanism of film crosslinking by UV (366 nm) exposure of an anthracene functional star polymer film and crosslinking was found to be imperative to forming stabilized porous films.

2.4. Photolithography of Honeycomb Films

Photolithography is a procedure which utilizes photons to transfer a pattern using a photo mask onto a photo-reactive substrate. The dimerization of anthracene moiety is well suited to this technology as the reversibility of the reaction is ideal for optical memory applications.[17–19]

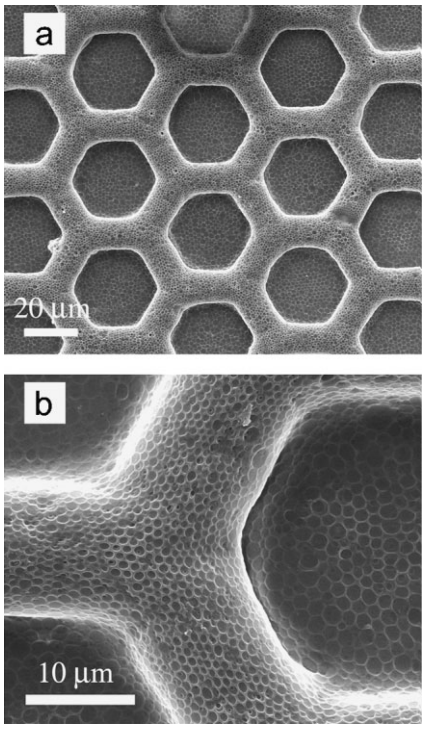

Figure 4. Honeycomb film, formed from poly(methyl acrylate) CCS polymer end-functionalized with anthracene. The film was photocrosslinked under 366 nm light and washed with THF. a) Low magnification; and b) high magnification.

Here, TEM grids are used as masks to create a new type of patterned material. The procedure is as follows, and is schematically represented in Figure 5. Anthracene functional honeycomb films are cast under standard BF conditions (Fig. 5a). A TEM grid is placed on the surface of this film, and irradiated with long wave UV (366 nm), thus crosslinking the exposed areas (Fig. 5b). Figure 6a shows the fluorescent micrograph of this structure, the darker areas are the crosslinked structures. Further, to demonstrate the reversibility of this process we removed the TEM grids and continued to irradiate the film with long wave UV (366 nm), effectively erasing the pattern formed (Fig. 5c). The TEM grid was then placed back on the surface and irradiated with short wave UV (254 mn), uncrosslinking the exposed areas (Fig. 5d). Figure 6b displays the fluorescent micrograph of this structure, the lighter regions from the pattern that has been rewritten into the porous film.

The patterned material as represented in Figures 5b and 6a, with crosslinked regions were then washed with THF to remove the uncrosslinked areas. Figure 7 shows the SEM micrographs of anthracene functional materials, photo- patterned as described above; these films were washed with THF after the initial photo-patterning steps, leaving the organic stable regions of the film. Figure 7a shows the patterned surface over a larger area and Figure 7b shows the center region highlighted in Figure 7a. Figures 7c and d show the crosslinked and uncrosslinked regions, respectively. Figure 7d indicates that

ADVANCED FUNCTIONAL MATERIALS

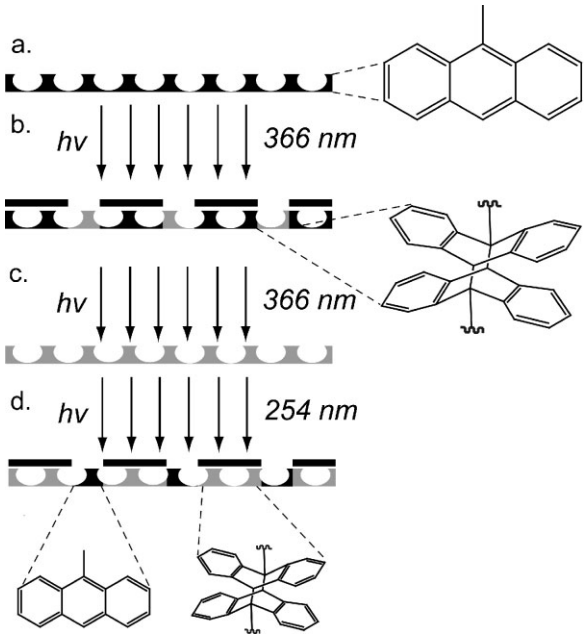

Figure 5. Schematic representation of photolithographic transfer using a TEM grid as a mask. a) As cast honeycomb film with fluorescent anthracene; b) photolithographic patterning of honeycomb films using a mask, crosslinking the exposed areas with 366 nm light; (c) removal of the mask and further irradiation with 366 nm light erases the pattern; and d) The TEM grid was then used again to rewrite into the film, this time with the 254 nm light therefore creating the inverse pattern.

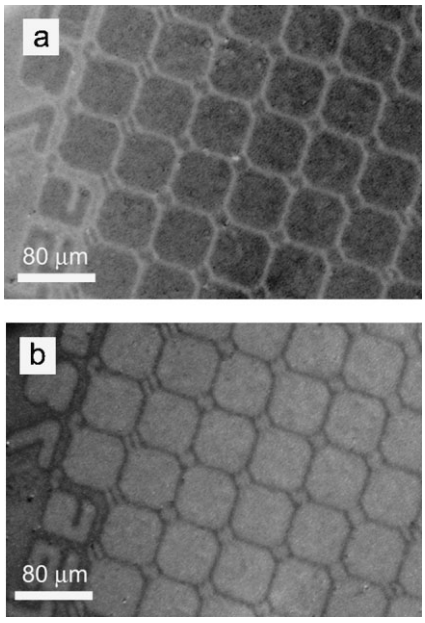

Figure 6. Fluorescent microscope images of photo-induced patterning of honeycomb films cast from anthracene functional poly(methyl acrylate) star polymer, using a TEM grids as a photo-mask. a) Initial irradiation with 366 nm light; b) this surface has been irradiated further without the TEM grid at 366 nm light, erasing the pattern shown in (a), the grid was the placed back on the film and then irradiated with 254 nm light.

the ''uncrosslinked'' area of the film has been successfully washed away.

The ability to generate honeycomb films that can be photo-patterned, in combination with conforming to non-planar substrates makes this process a very powerful technique. We envisage that honeycomb films could be coated in existing platforms (e.g., microfluidic channels), crosslinked in the area where the film is desired and the non-irradiated material simply removed by washing. The synthetic strategy outlined in this manuscript also allows facile incorporation of other functionalities (e.g., biospecific) which could lead to new bio-sensor technologies.

We have demonstrated that by utilizing an anthracene functional PMA star polymer, with its low T_g (giving rise to flexibility), and its reversible photocrosslinkable moiety, a range of patterns can be generated. Micrometer-sized pores ordered in an hexagonal pitch can be prepared using the BF technique. A 3D pattern originating from a TEM grid can be created by contouring the honeycomb film over the surfaces of the

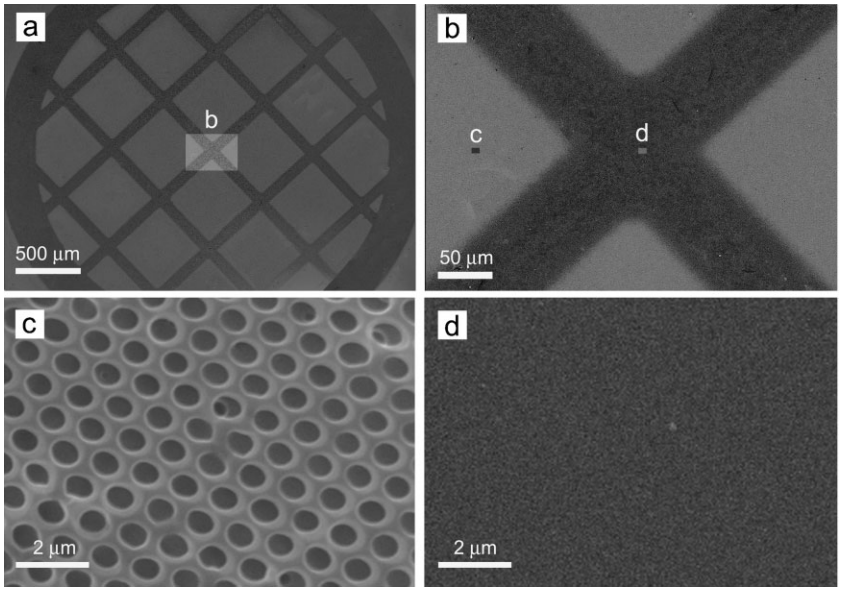

Figure 7. Scanning electron micrographs of photo-patterned honeycomb materials. Anthracene functional PMA star polymer was cast under BF conditions and a TEM grid was then placed onto the surface and the film was placed under 366 nm UV light to crosslink the exposed areas. This film was then washed with THF to remove the uncross-linked material, leaving the TEM-grid induced pattern; a) low magnification displaying the pattern from TEM grids; b) medium magnification of area highlighted in (a); c) high magnification of area highlighted in (b) showing where honeycomb structure remains; d) high magnification of area highlighted in (b) highlighting the area where the honeycomb structure has been washed away.

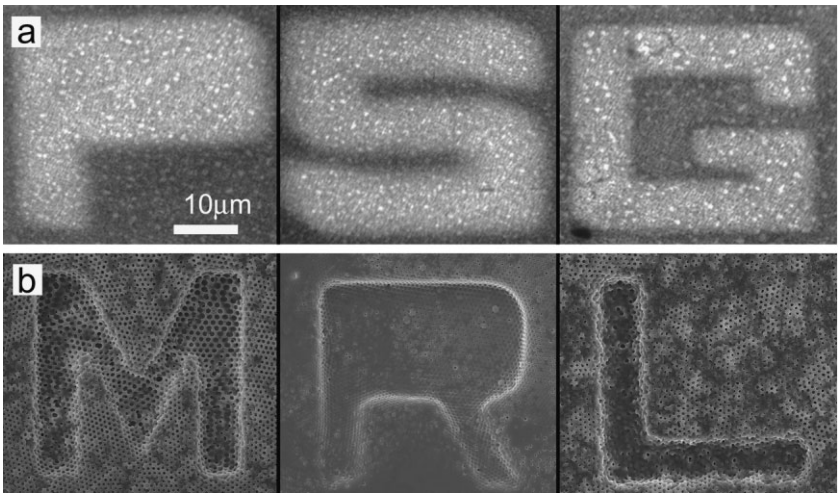

Figure 8. Top line; Letters ''PSG'' (Polymer Science Group) generated utilizing a TEM grid as a photo-mask and visualized with fluorescent microscopy. Bottom line; the letters ''MRL'' (Materials Research Laboratory) generated using a TEM grid as a substrate for honeycomb formation, visualized by SEM.

grid. Furthermore, at the molecular level through the reversible photo-dimerization of the anthracene end group, another pattern can be generated. To highlight these patterning technologies we utilized a TEM grid, containing coordinates, as a mask to pattern using both these strategies – 2D photolithography and 3d conformal replications – with the same honeycomb films. Figure 8a displays the results visualized by fluorescent microscopy, showing the letters ''PSG'' generated via photolithography. Unfortunately the size of the pores is out of the resolution of the fluorescent microscope therefore they are not visualized; however the pattern induced by photolithography is clearly visualized. Figure 8b displays the letters ''MRL'' generated from the unique conformal replication of the grid with an ordered honeycomb film, where the letters ''MRL'' and the porous morphology is also clearly visible. The dimensions of the topographic features can be used to control the final porous structure. With narrow features as observed in the ''M'' the pores are stretched and a larger diameter is observed. Larger features such as that observed in the ''R'' structure the pores are not stretched and are more homogenous.

3. Conclusions

Anthracene functional star polymers with a low T_g can create multifaceted porous materials which have great potential in a range of applications. Core crosslinked star polymers based on poly(methyl acrylate), with two hydroxyl groups per arm, were prepared by the ''arm first'' strategy. These hydroxyl groups were reacted with 9-anthracene carbonyl chloride to yield star polymers with two anthryl groups per arm. This star polymer can form porous films by the BF technique, on flat, and on non-flat substrates, because of its low T_g and star structure. The anthracene functional honeycomb films were reversible photocrosslinked, through the dimerization of anthracene groups. This crosslinking reaction was used, not only to create organic-stable films, but also to create honeycomb films with an additional level of patterning, showing the multifaceted nature of these honeycomb films. The techniques and methods established in this work will greatly enhance the applicability of these films in areas which have stringent, multiple requirements; such as, microfluidics, microreactors and biosensors.

4. Experimental

Materials: All chemicals were purchased from Sigma–Aldrich unless otherwise stated. Methyl acrylate (MA, 99%) was passed over an aluminum oxide (basic) column immediately prior to use. *N*,*N*,*N*′,*N*″,*N*″-pentamethyldiethylenetriamine (PMDETA, 99%) was distilled from calcium hydride. Divinyl benzene (DVB, 80% mixture of isomers) and ethylene glycol dimethacrylate (EGDMA, 98%) monomers were washed 3 times with 5% sodium hydroxide solution and once with distilled water, the solutions were dried over $MgSO_4$, filtered and distilled from calcium hydride. 2-(2′-Bromo-2′-methylpropanoyloxy)ethyl 2,2,5-trimethyl-1,3-dioxane-5-carboxylate (1) [30] was synthesized by a previously reported procedure. 9-Anthracenecarboxylic acid (99%), 4-dimethylaminopyridine (DMAP, 99+ %), anisole (anhydrous, 99+ %), tetrahydrofuran (THF, anhydrous, 99+ %), thionyl chloride ($SOCl_2$, 99+ %), and copper (I) bromide (CuBr, 98%) were used without further purification.

Methods: Gel permeation chromatography (GPC) was performed on a Shimadzu system with a Wyatt DAWN DSP multiangle laser light scattering (MALLS) detector (690 nm, 30 mW) and a Wyatt OPTILAB EOS interferometric refractometer (690 nm). Tetrahydrofuran (THF) was used as the eluent with three Phenomenex phenogel columns (500, 10^4, and 10^6 Å porosity; 5 μm bead size) operated at 1 mL min^{-1} with the column temperature set at 30 °C. Astra software (Wyatt Technology Corp.) was used to process the data using known d*n*/d*c* values to determine the molecular weight or an assumption of 100% mass recovery of the polymer where the d*n*/d*c* value was unknown. Scanning electron microscopy (SEM) was conducted on XL 30 Philips Head SEM. Samples were coated with a gold coating using a Dynavac Mini Sputter Coater prior to imaging. Differential scanning calorimetry (DSC) was performed on a TA 2920 modulated DSC equipped with an LNCA cooling system. Measurements were repeated three times with data taken on the second run. Temperature range was varied according to the literature T_g value of the polymer being measured, the rate was kept constant at 10 °C min^{-1}. Confocal microscopy experiments were performed on a Leica TCS-SP2 confocal laser scanning microscope using a Picoquant 405-nm pulsed diode laser as the excitation source. Fluorescence spectra were collected on an SPEX Fluorolog-Tau2 spectrofluorometer (Jobin Yvon), using a detection angle of 90° from the direction of the excitation beam. The excitation wavelength was 355 nm and the scan range was 380–800 nm in 3 nm steps, integrating at 1s per point.

Synthesis of Poly(methyl acrylate) Macroinitiator: A mixture of MA (15.69 mL, 0.15 mol), CuBr (166 mg, 1.10 mmol), PMDETA

ADVANCED FUNCTIONAL MATERIALS

(484 μL, 2.30 mmol) and 2-(2′-Bromo-2′-methylpropanoyloxy)ethyl 2,2,5-trimethyl-1,3-dioxane-5-carboxylate (1) (430 mg, 1.10 mmol) was added to a Schlenk flask and degassed by three freeze-pump-thaw cycles. The flask was then immersed in an oil bath at 80 °C and heated for 2 h. The reaction mixture was diluted with THF (100 mL), passed through a column of basic alumina and celoite (4:1) and precipitated into methanol. The precipitate was collected by vacuum filtration and analyzed by GPC-MALLS (67% yield, $M_n = 7.00 \times 10^3$ g mol^{-1}, PDI = 1.10) ^{1}H NMR spectroscopy ($CDCl_3$, δ):1.19 (s, 6H, CH_3), 1.35 (s, 3H, CH_3), 1.40 (s, 6H, CH_3), 1.79–1.98 (br, 2H, CH_2), 2.27–2.45 (br, 1H, CH), 2.73 (m, 2H, CH_2), 3.59–3.72 (br, 3H, CH_3), 3.98 (d, 2H, CH_2), 4.22 (d, 2H, CH_2), 4.35 (m, 2H, CH_2).

Synthesis of Core Crosslinked Star Poly(methyl acrylate-co- divinyl benzene): A mixture of PMA macroinitiator ($M_n = 7.00 \times 10^3$ mol^{-1}, 300 mg, 0.04 mmol), DVB (91.5 μL, 0.60 mmol), CuBr (6.0 mg, 0.04 mmol), PMDETA (20 μL, 0.08 mmol) in anisole (2.50 mL) was added to a Schlenk flask and degassed by three freeze-pump-thaw cycles. The flask was then immersed in an oil bath at 100 °C and heated for 40 h. The mixture was diluted with THF (100 mL), passed through a column of basic alumina and celite (4:1), concentrated and precipitated into cold methanol (250 mL) and collected by filtration to afford a colorless solid, which was analyzed by GPC-MALLS ($M_n = 3.80 \times 10^5$ g mol^{-1}, PDI = 1.23, no. arms = 36). ^{1}H NMR spectroscopy ($CDCl_3$, δ): 1.19 (s, 6H, CH_3), 1.35 (s, 3H, CH_3), 1.40 (s, 6H, CH_3), 1.79–1.98 (br, 2H, CH_2), 2.27–2.45 (br, 1H, CH), 2.73 (m, 2H, CH_2), 3.59–3.72 (br, 3H, CH_3), 3.98 (d, 2H, CH_2), 4.22 (d, 2H, CH_2), 4.35 (m, 2H, CH_2).

Deprotection of Acetonide Functional PMA Star Polymers: Acetonide-protected star polymers (200 mg) were dissolved in 20.0 ml of THF: Methanol (2:3). Dowex, H^+ resin (1.0 g) was added, and the reaction mixture was stirred for 18 h at 50 °C. The reaction mixture was filtered to remove the acidic resin. The methanol and THF were then removed by rotary evaporation, and finally dried under high vacuum. ^{1}H NMR spectroscopy ($CDCl_3$, δ): 1.19 (s, 6H, CH_3), 1.35 (s, 3H, CH_3), 1.79–1.98 (br, 2H, CH_2), 2.25–2.46 (br, 1H, CH), 2.73 (m, 2H, CH_2), 3.59–3.72 (br, 3H, CH_3), 3.84 (s, 4H, CH_2), 4.35 (m, 2H, CH_2).

Preparation of 9-Anthracene Carbonyl Chloride (2): An aliquot of $SOCl_2$ (10.0 mL, 0.21 mol) was placed in a N_2-purged flask followed by the addition of 9-anthracenecarboxylic acid (1.0 g, 4.5 mmol). One drop of anhydrous dimethylformamide was added, and the reaction was heated (60 °C) under reflux for 18 h. Excess $SOCl_2$ was evaporated under reduced pressure to yield the final product as yellow solid (1.0 g, 93% yield). ^{1}H NMR spectroscopy ($CDCl_3$, δ): 7.52 (m, 4H, CH), 7.59 (m, 2H, CH), 8.03 (d, 1H, CH), 8.09 (d, 1H, CH), 8.56 (s, 1H, CH).

Functionalization of Hydroxyl-Functional Star Polymers with Anthracene: 9-anthracene carbonyl chloride (2) (100 mg, 0.40 mmol) and DMAP (10 mg, 0.10 mmol) were dissolved in anhydrous THF (1.0 mL). Hydroxyl functional PMA star polymer (150 mg) was dissolved in a mixture of dry pyridine (500 μL) and anhydrous THF (5.0 mL) and added drop-wise to the reaction mixture, the reaction was stirred for 18 h at room temperature. The solution was filtered and the solvents evaporated under reduced pressure. The polymer was redissolved in minimum THF and precipitated into methanol (150 mL) and collected by filtration to afford a pale yellow solid. ($M_n = 3.81 \times 10^5$ g mol^{-1}, PDI = 1.23, no. arms = 36). ^{1}H NMR spectroscopy ($CDCl_3$, δ): 1.19 (s, 6H, CH_3), 1.35 (s, 3H, CH_3), 1.79–1.98 (br, 2H, CH_2), 2.27–2.45 (br, 1H, CH), 2.73 (m, 2H, CH_2), 3.59–3.72 (br, 3H, CH_3), 4.35 (m, 2H, CH_2), 4.49 (s, 4H, CH_2), 7.5–8.3 (m, ArH).

Honeycomb Film Preparation: A drop (20 μL) of anthracene functional star-polymer solution in benzene (10 g L^{-1}) was cast onto a surface (glass cover slip or TEM grid). A humidified flow (70% R.H., 25 °C) of air was directed onto this droplet at a rate of 3 L min^{-1}. The solution formed an opaque surface within seconds and the solvent was evaporated within 45 seconds. The film was then allowed to dry at 20 °C and 30% R.H. overnight.

Reversible Crosslinking of Anthracene Functional Honeycomb Films: The PMA honeycomb material was placed in a vial, degassed with argon and placed under a UV lamp (4 h, 366 nm light at 5 W) 3 cm from source. The decrease in fluorescence intensity was monitored by florescence spectroscopy. To reverse the crosslinking reaction the film was placed under a UV lamp (4 h, 254 nm light at 5 W) 3 cm from the source. These photo-patterned surfaces were analyzed by fluorescence microscopy. In some instances these films were then washed with THF to remove the uncrosslinked materials and analyzed by SEM.

Received: March 3, 2008
Revised: June 27, 2008
Published online: October 6, 2008

[1] Y. Wang, A. S. Angelatos, F. Caruso, *Chem. Mater.* **2008**, *20*, 848.
[2] S. A. Jenekhe, L. X. Chen, *Science* **1999**, *283*, 372.
[3] G. Widawski, M. Rawiso, B. Francois, *Nature* **1994**, *369*, 387.
[4] L. A. Connal, P. A. Gurr, G. G. Qiao, D. H. Solomon, *J. Mater. Chem.* **2005**, *15*, 1286.
[5] L. A. Connal, G. G. Qiao, *Adv. Mater.* **2006**, *18*, 3024.
[6] L. A. Connal, G. G. Qiao, *Soft Matter* **2007**, *3*, 837.
[7] L. A. Connal, *Aust. J. Chem.* **2007**, *60*, 794.
[8] L. A. Connal, R. Vestberg, P. A. Gurr, C. J. Hawker, G. G. Qiao, *Langmuir* **2008**, *24*, 556.
[9] J. S. Park, S. H. Lee, T. H. Han, S. O. Kim, *Adv. Funct. Mater.* **2007**, *17*, 2315.
[10] D. Y. Ryu, K. Shin, E. Drockenmuller, C. J. Hawker, T. P. Russell, *Science* **2005**, *308*, 236.
[11] B. Gotsmann, U. Duerig, J. Frommer, C. J. Hawker, *Adv. Funct. Mater.* **2006**, *16*, 1499.
[12] E. Drockenmuller, L. Y. T. Li, D. Y. Ryu, E. Harth, T. P. Russell, H. C. Kim, C. J. Hawker, *J. Polym. Sci. Part A* **2005**, *43*, 1028.
[13] H. Yabu, M. Tanaka, K. Ijiro, M. Shimomura, *Langmuir* **2003**, *19*, 6297.
[14] B. Erdogan, L. Song, J. N. Wilson, J. O. Park, M. Srinivasarao, U. H. F. Bunz, *J. Am. Chem. Soc.* **2004**, *126*, 3678.
[15] T. Kabuto, Y. Hashimoto, O. Karthaus, *Adv. Funct. Mater.* **2007**, *17*, 3569.
[16] B. de Boer, U. Stalmach, H. Nijland, G. Hadziioannou, *Adv. Mater.* **2000**, *12*, 1581.
[17] O. Karthaus, Y. Hashimoto, K. Kon, Y. Tsuriga, *Macromol. Rapid Commun.* **2007**, *28*, 962.
[18] M. F. Montague, C. J. Hawker, *Chem. Mater.* **2007**, *19*, 526.
[19] H. D. Becker, *Chem. Rev.* **1993**, *93*, 145.
[20] H. Bouas-Laurent, A. Castellan, J. P. Desvergne, R. Lapouyade, *c, Chem. Soc. Rev.* **2000**, *29*, 43.
[21] D. S. Tyson, C. A. Bignozzi, F. N. Castellano, *J. Am. Chem. Soc.* **2002**, *124*, 4562.
[22] T. D. Trouts, D. S. Tyson, R. Pohl, D. V. Kozlov, A. G. Waldron, F. N. Castellano, *Adv. Funct. Mater.* **2003**, *13*, 398.
[23] J. Matsui, K. Abe, M. Mitsuishi, T. Miyashita, *Mol. Cryst. Liq. Cryst.* **2004**, *424*, 187.
[24] W. A. Goedel, R. Heger, *Langmuir* **1998**, *14*, 3470.
[25] B. S. Sandanaraj, R. Demont, S. V. Aathimanikandan, E. N. Savariar, S. Thayumanavan, *J. Am. Chem. Soc.* **2006**, *128*, 10686.
[26] T. Ihara, T. Fujii, M. Mukae, Y. Kitamura, A. Jyo, *J. Am. Chem. Soc.* **2004**, *126*, 8880.
[27] Y. Chujo, K. Sada, R. Nomura, A. Naka, T. Saegusa, *Macromolecules* **1993**, *26*, 5611.
[28] Y. Zheng, M. Micic, S. V. Mello, M. Mabrouki, F. M. Andreopoulos, V. Konka, S. M. Pham, R. M. Leblanc, *Macromolecules* **2002**, *35*, 5228.
[29] For synthesis of CCS polymers see: a) S. Abrol, P. A. Kambouris, M. G. Looney, D. H. Solomon, *Macromol. Rapid Commun.* **1997**, *18*, 755. b) S. Abrol, M. J. Caulfield, G. G. Qiao, D. H. Solomon, *Polymer*

2001, *42*, 5987. c) A. W. Bosman, R. Vestberg, A. Heumann, J. M. J. Frechet, C. J. Hawker, *J. Am. Chem. Soc.* **2003**, *125*, 715. d) P. A. Gurr, G. G. Qiao, D. H. Solomon, S. E. Harton, R. J. Spontak, *Macromolecules* **2003**, *36*, 5650. e) J. Xia, X. Zhang, K. Matyjaszewski, *Macromolecules* **1999**, *32*, 4482. f) H. Gao, S. Ohno, K. Matyjaszewski, *J. Am. Chem. Soc.* **2006**, *128*, 15111. g) K. Y. Baek, M. Kamigaito, M. Sawamoto, *Macromolecules* **2001**, *34*, 215. h) T. Terashima, M. Ouchi, T. Ando, M. Kamigaito, M. Sawamoto, *Macromolecules* **2007**, *40*, 3581. i) J. T. Wiltshire, G. G. Qiao, *Macromolecules* **2006**, *39*, 4282. j) J. T. Wiltshire, G. G. Qiao, *Macromolecules* **2006**, *39*, 9018.

[30] L. A. Connal, R. Vestberg, C. J. Hawker, G. G. Qiao, *Macromolecules* **2007**, *40*(22), 7855.